Identification of radiative transitions in highly porous silicon

LETTER TO THE EDITOR

Identification of radiative transitions in highly porous silicon

P D J Calcott, K J Nash, L T Canham, M J Kane and D Brumhead

Defence Research Agency (RSRE), St Andrews Road, Malvern, Worcs WR14 3PS, UK

Abstract. We report time-resolved photoluminescence spectroscopy of highly porous silicon. Our results show that the luminescence is due to localized quantum-confined excitons in undulating crystalline silicon wires. The resonantly excited photoluminescence spectrum exhibits satellite structure due to momentum-conserving phonons of crystalline silicon. This provides a clear signature of the crystalline-silicon electronic band structure. The spin states of the localized exciton are split by the electron–hole exchange interaction. This splitting is manifested both in the strong dependence of the luminescence lifetime on temperature, and as an energy gap in the resonantly excited photoluminescence spectrum. The experimental splitting is in good agreement with the value calculated for a localized exciton in crystalline silicon.

The demonstration [1] of efficient visible luminescence from highly porous Si has stimulated a great deal of interest. The attribution of this luminescence to quantum-confined carriers in crystalline Si wires [1] has been supported by transmission electron microscopy [2] (TEM) which shows the structure to consist of undulating columns of crystalline Si. First-principles calculations [3] for wires of the dimensions observed in TEM account for both the quantum upshift of the luminescence energy and the radiative lifetimes. We report time-resolved photoluminescence (PL) spectroscopy which confirms the model of quantum confinement in crystalline Si. Our experiments show that the radiative states, even at room temperature, are localized excitons with a large exchange splitting. Our observation of momentum-conserving phonon satellites provides clear evidence that the excitons are located in crystalline Si.

The detailed results relevant to this paper come from studies of two samples. The first, called A in this work and no 4 in [2], was studied by TEM. The second, B, was studied optically. Both were prepared by anodization of p-type Si (resistivity 40 Ω cm) at 20 mA cm^{-2} for 5 min in 20% ethanoic HF, either immediately before measurement (A), or two years prior to detailed measurement (B). Surface oxidation of B over the period before measurement produced a more photostable structure and a greater quantum upshift than in A [4]. The porosity of the fresh layers was 80%, and TEM of sample A indicates [2] a crystalline Si wire structure with variations of thickness on a length scale of ~ 40 Å. The average wire width is ~ 30 Å, and the thickness variations are ± 10 Å. PL was excited with argon or dye laser light and time-resolved measurements were performed with an acousto-optic modulator, photomultiplier and a gated photon counter. Spectral lineshapes were corrected by reference to a calibrated source.

We found that the PL spectrum consists of two overlapping bands with quite different lifetimes, marked S (slow) and F (fast) in figure 1. Band S, which comprises 97% of the CW intensity, is the subject of most of our experiments and has properties similar to those reported by others [5,6]. The lifetime of S (τ_S) is wavelength-dependent and $\sim 30\,\mu$s at room temperature. Band F, which has not previously been reported, has a lifetime faster than our experimental resolution of ~ 30 ns, and comprises only 3% of the intensity. Discussion of band F will be deferred to a comprehensive publication. Figure 2(*a*) shows time-resolved PL in the high-energy tail of the PL spectrum, and clearly shows the two components of the PL, S and F. The decay of band S is not a single exponential, but rather a distribution and so as in [6] we have taken the term lifetime to mean the time taken for the PL to decrease by a factor of e. We measured τ_S at various PL photon energies in the range 1.7 eV to 2.4 eV, and over the temperature (T) range 2 K–287 K. Figure 2(*b*) plots $\ln(\tau_S)$ versus $1/T$ and shows that the variation of τ_S can be accurately fitted by modelling the initial states of PL as a two-level system with energy splitting Δ and lifetimes τ_L (lower state) and τ_U (upper state). Figure 2(*c*) plots the level splitting Δ (extracted from the fit) against PL energy. Figure 2(*d*) plots τ_U and τ_L in the same way. τ_L is always much larger than τ_U.
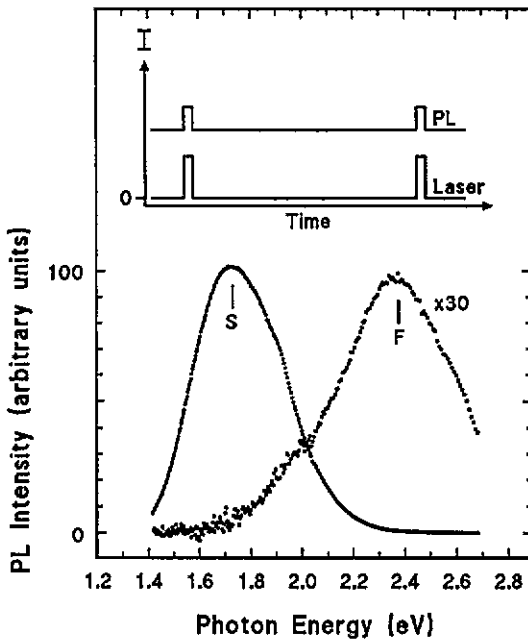

Figure 1. The 300 K PL spectrum of sample B. Bands S and F have different lifetimes, τ_S and τ_F respectively (see text). The CW spectrum is the sum of S and F. To differentiate between S and F, the period of the laser pulses was chosen to be much smaller than τ_S and much larger than τ_F. The inset shows the laser pulse and PL signal in these circumstances. The S band PL is the almost constant background, while the F band PL is the additional signal present during the laser pulse. The intensity of the F band PL is determined by the appropriate subtraction of gated signals. Excitation was with a mean power density of 20 mW cm^{-2} of 2.708 eV laser light and a 1:12 mark to space ratio.

We also measured band S at low temperature (2 K) with selective laser excitation. PL spectra were measured for excitation energies $\hbar\omega_l$ in the range 1.8 eV to 2.5 eV. Figure 3 shows PL spectra as a function of $\hbar\omega_l - \hbar\omega_p$ (where $\hbar\omega_p$ is the PL photon energy), which is the sum of the energy lost by the excitons when they relax from the photocreated state to the luminescent state, and the energy lost to the lattice if the optical transitions are phonon-assisted. Thus figures 3(*a*), (*b*) can be interpreted as energy-loss spectra. Figure 3(*a*) shows that there is very little PL until a certain minimum value of energy loss is reached, following which the PL intensity increases
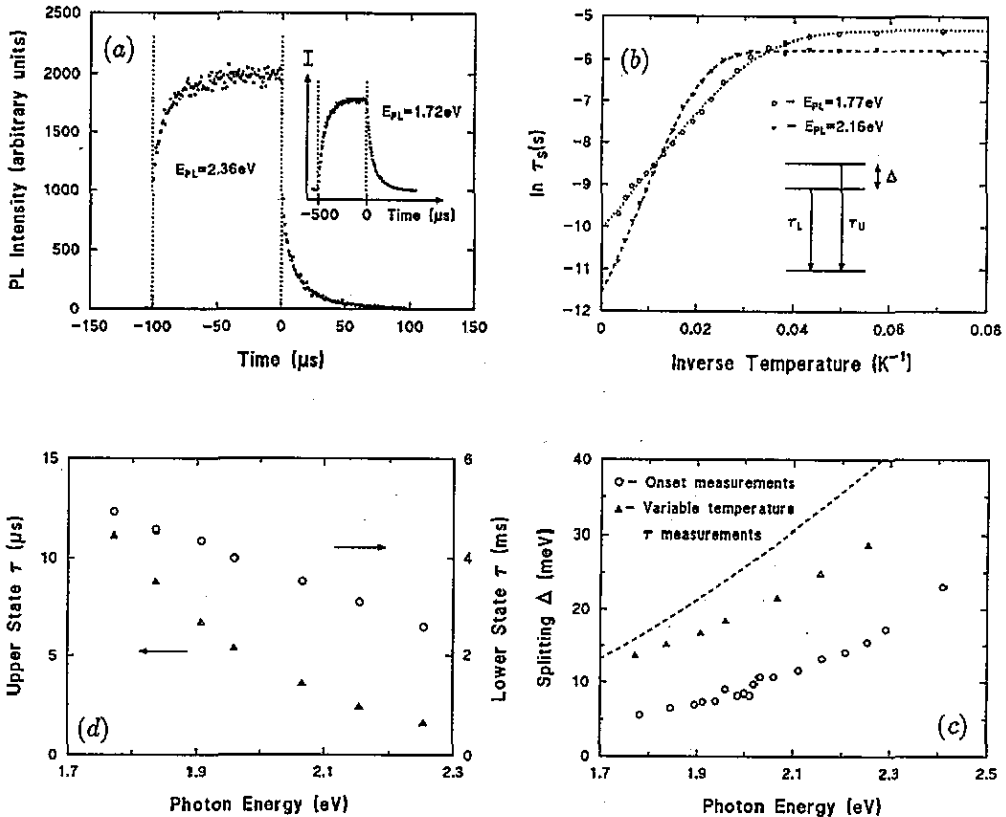
Figure 2. (*a*) Typical time-resolved PL at 300 K. The discontinuous increase and decrease in the PL intensity corresponding to the start and end of the laser pulse (dashed lines) are due to band F, which is of intensity comparable to band S at this photon energy. For comparison, a similar measurement at the peak PL energy is included in the inset, and at this energy, band F is absent (cf figure 1). Excitation was with a mean power density of 20 mW cm^{-2} of 2.708 eV laser light and a 1:1 mark to space ratio. (*b*) The temperature dependence of τ_S, the lifetime of band S. Each broken line is the fit of the data at a single PL energy to the model of a thermal-equilibrium two-level system with the upper-level lifetime τ_U, lower-level lifetime τ_L and energy splitting Δ of the levels as adjustable parameters. The ratio of the lower-state to upper-state degeneracies is assumed to be three. The fit is very good for each PL energy measured (these energies are given by the ordinates of the points plotted in figure 2(*d*)). (*c*) The energy splitting Δ of the luminescent states derived from the fit to the temperature-dependence of τ_S (triangles), and from the onset of selectively excited PL (circles). The difference between the values of Δ obtained by the two methods is discussed in the text. The dashed curve is the exchange splitting calculated in a simple effective-mass theory with no adjustable parameters (see text). (*d*) The lifetimes of the upper and lower luminescent states which contribute to band S. These values are derived from the fit to the temperature-dependence of τ_S.

sharply. The value of this onset energy is plotted in figure 2(*c*) as a function of laser energy. Raising the temperature smears out the PL spectrum, and the onset is not discernible above 50 K. At larger values of $\hbar\omega_l - \hbar\omega_p$, two further onsets are observed (figure 3(*b*)).

We propose the following theory to explain these results. The PL band S arises
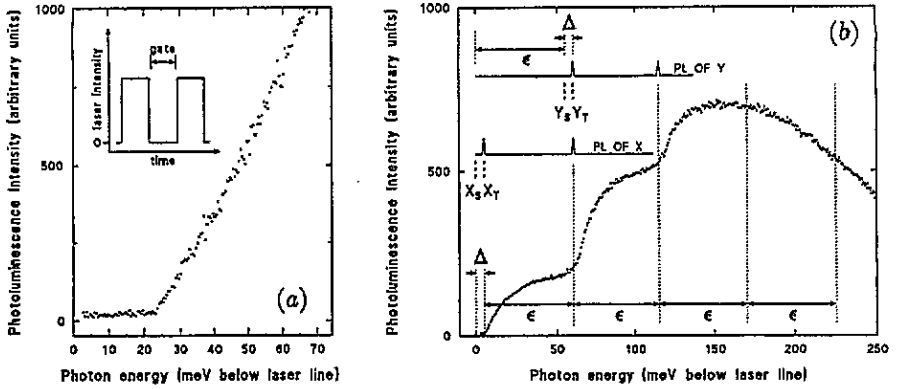
Figure 3. (a) An example of the PL spectrum observed at 2 K with selective excitation. The inset shows the time gating used, with PL only being measured during the times when the laser is not illuminating the sample. Thus the measured intensity is that of the S band only, with no contribution from the F band. Excitation was with a mean power density of 1 W cm^{-2} of 2.410 eV laser light and a 1:1 mark to space ratio. Note the onset of PL at an energy loss of 23 meV. (b) The PL spectrum recorded at 2 K for a larger range of energy loss, with a laser energy $\hbar\omega_l$ of 1.819 eV and a mean power density of 3 W cm^{-2}. There are three strong onsets. The first of these has the same form as the onset shown in figure 3(a), but occurs at a smaller value of energy loss, because $\hbar\omega_l$ is smaller (figure 2(c)). The second and third onsets occur at energies ϵ, 2ϵ below the first, where $\epsilon = 56.3 \pm 1.1$ meV. There are no onsets at higher multiples of ϵ. This behaviour is observed for $\hbar\omega_l$ in the range 1.782 eV to 2.410 eV, corresponding to first-onset energies from 5.6 meV to 23 meV (figure 2(c)). The strength of the second and third onsets relative to the first decreases with increasing $\hbar\omega_l$, and is very small at $\hbar\omega_l = 2.410$ eV. We propose an explanation in terms of the absorption and PL processes shown in the inset. The energies of the exciton states that are involved in these transitions are marked with dashed lines. Zero-phonon absorption occurs into the singlet component X_S of the discrete bound exciton state X, while phonon-assisted absorption occurs into the singlet component Y_S of the discrete bound exciton state Y. These absorption processes are followed by relaxation into the triplet states X_T and Y_T respectively, and then by either zero-phonon or phonon-assisted PL. The phonon-assisted processes involve momentum-conserving phonons of crystalline Si. The PL spectrum consists of onsets rather than sharp peaks because Δ is the *minimum* value of energy that the exciton can lose by relaxation.

from the recombination of localized excitons which have an exchange splitting that is dramatically enhanced by quantum confinement. The excitons are localized (even at room temperature) and given a considerable inhomogeneous PL linewidth [7] by the thickness variations of the wires. The orbital degeneracy of the bulk Si valence band is completely lifted by quantum confinement [3], because the masses for different valence-band Bloch orbitals are different. Thus both the electron and hole have spin $\frac{1}{2}$. Each localized exciton state is split by the exchange interaction [8] into a spin singlet and a spin triplet, with the triplet lower in energy. This leads to an immediate explanation of the T-dependence of τ_S. The upper and lower states used to fit τ_S are the singlet and triplet respectively, and Δ is the exchange splitting. The lifetimes τ_L and τ_U are also explained. The singlet lifetime τ_U is in reasonable agreement with first-principles calculations [3]. The radiative lifetime for a pure triplet state would be infinite, but the spin–orbit interaction mixes some singlet character into the triplet state making transitions weakly allowed.

The minimum energy loss (first onset energy) observed in selectively excited PL also has a simple interpretation. Excitons are predominantly photocreated in a singlet rather than a triplet state because the absorption strength is inversely proportional to the radiative lifetime and the singlet is 400 to 1200 times faster than the triplet, depending on the photon energy (figure 2(*d*)). At 2 K the thermal energy of the carriers ($kT = 0.17$ meV) is negligible compared to Δ and so, following relaxation, the PL arises from the triplet state only. The first PL onset observed in the energy-loss spectrum (figure 3(*a*)) arises because the (fast) singlet states into which an exciton can be photocreated have a minimum energy separation from the (slow) triplet state which the same exciton occupies, after relaxation, when it recombines. This minimum energy separation is the exchange splitting Δ. The value of Δ deduced from the first onset differs from that deduced from $\tau_S(T)$ (figure 2(*c*)) for the following reason. The luminescent excitons with a particular quantum upshift are confined by wires with a variety of shapes and sizes, and thus although these excitons have the same energy, they have a distribution of wavefunctions and exchange splittings. The first onset measured in the 2 K PL spectrum corresponds to the minimum Δ-value of the distribution, whereas the energy splitting deduced from τ_S is a weighted average. The first onset energy observed in the PL spectrum exists only when most of the PL comes from the triplet state. When T is raised to 50 K the singlet and triplet PL have comparable intensity and the first onset disappears. The optically detected magnetic resonance (ODMR) of the PL band behaves similarly. At low T, a resonance consistent with a triplet state is observed [9]. The ODMR intensity decreases strongly with increasing T, and is unobservable at 80 K [9], consistent with the relative strengths of the singlet and triplet PL in our theory.

The second and third PL onsets (figure 3(*b*)) can only be explained in terms of absorption and PL processes assisted by momentum-conserving phonons in crystalline Si (inset to figure 3(*b*)). The bulk-Si crystal momentum that is conserved in such processes remains well defined because the dimensions of the quantum wires amount to many bulk Si primitive cells. The properties of quantum-confined excitons in crystalline Si wires closely mirror those of excitons localized at point defects in bulk Si [10]. Thus our theory explains why

(i) $\epsilon = 56.3 \pm 1.1$ meV, since, within experimental error, this equals the 57.3 ± 0.4 meV energy of the Si TO(Δ) phonons [11],

(ii) coupling at other phonon energies is weak, since only the TO(Δ) phonons give efficient phonon-assisted transitions [10],

(iii) the first onset, rather than the laser line, is replicated,

(iv) there are precisely two phonon satellites, since, for a momentum-conserving phonon, the absorption and PL processes each have precisely one strong phonon satellite [10], and

(v) the relative strength of the phonon coupling decreases with increasing laser energy, since the zero-phonon transition rate increases rapidly with increasing carrier confinement ([3, 10] and figure 2(*d*)).

We emphasize that the number of phonon satellites, precisely two, demonstrates that the phonons are momentum-conserving phonons. Alternative interpretations, involving multiphonon (Huang–Rhys) satellites [12], or a hot-exciton cascade [13, 14], are inconsistent with the observation of precisely two phonon satellites: if the first two satellites are strong, then strong higher-order satellites should also be observed.

Both the value of the experimental energy splitting Δ and its trend with photon

energy are consistent with the exchange splitting calculated in effective-mass theory (EMT) for localized quantum-confined excitons in undulating crystalline Si wires. EMT gives [8] $\Delta = J \int d^3r |\varphi(r,r)|^2$ where $\varphi(r_e, r_h)$ is the envelope function for the exciton and J is twice the exchange integral per unit inverse volume for the conduction-band-minimum and valence-band-maximum states in bulk Si. We obtain a preliminary estimate of J as 7.0×10^{-26} meV m^3, from the 2.9 meV exchange splitting of the Ga-2 isoelectronic donor [15] in bulk Si and the donor variational wavefunction of [16], whose accuracy has been demonstrated by Faulkner [17]. For porous Si we first consider the PL peak at $\hbar\omega_p = 1.72$ eV, assuming that the initial state is an exciton localized at a typical local maximum in wire width (minimum in energy). Such a fluctuation is most easily approximated as a sphere of diameter D. In the fresh sample A, TEM [2] shows that $D \sim 35$ Å. The increased quantum upshift of PL in the aged sample B is due to surface oxidation, which reduces the size of the crystalline Si regions in which the carriers are confined. Following [3], D is reduced by ~ 5 Å. φ is taken to be that for an electron and hole perfectly confined to the sphere, neglecting correlation. This gives $\Delta = 13.9$ meV. This value is dramatically enhanced over the < 0.15 meV exchange splitting for the free exciton in bulk Si [18] both by quantum confinement and because the states of the latter exciton are not eigenstates of spin. To calculate Δ at other PL energies we assume that the localized excitons at different energies are confined in structures that have the same shape and that differ only in length scale L. Neglecting the electron–hole interaction and deviations from EMT, the upshift due to quantum confinement is proportional to L^{-2}, while the exchange splitting is proportional to L^{-3}. Figure 2(c) shows the resulting relation $\Delta \propto (\hbar\omega_p - E_g)^{1.5}$ where $E_g = 1.17$ eV is the 2 K band gap energy of bulk Si and the constant of proportionality is fixed by the calculation at $\hbar\omega_p = 1.72$ eV. The calculated exchange splittings are clearly comparable to the experimental values, and exhibit the same trend with $\hbar\omega_p$, although exact agreement with experiment is not expected given the approximations that we have made.

There is no natural explanation of the energy splitting Δ as anything other than an exchange splitting. Δ is much smaller than the energy splitting of states with different confinement or Coulomb energies, since these energies are large for quantum-confined states in narrow (~ 30 Å) wires. Thus excitation energies corresponding to different envelope functions, e.g. intersubband excitation energies [3], or binding energies of excitons [3, 19], donors or acceptors are expected to be 100 meV or larger. The small energy splitting Δ can only correspond to a weak perturbation which lifts the degeneracy of exciton states with the same envelope function. Within the model of localized quantum-confined excitons in a crystalline Si structure, excitons have spin degeneracy and conduction-band valley degeneracy only. The perturbations that lift these degeneracies are the electron–hole exchange interaction and the valley–orbit interaction respectively. Studies of the PL at 2 K in magnetic field (B) confirm that Δ is the exchange splitting and not an orbital splitting. At $B = 9.6$ T the lifetimes and intensity were the same as at $B = 0$, the first onset of band S was still clearly visible and the PL was weakly circularly polarized. If Δ is the exchange splitting, then the luminescent state at 2 K is the spin triplet, and the only effect of the magnetic field on the inhomogeneously broadened PL band is to induce circular polarization. However when the environment of the exciton has low symmetry, as it does in porous Si, the degree of circular polarization is expected to be weak, in agreement with our experiments. Weak circular polarization is also found for triplet excitons localized at defect complexes in bulk Si [20]. The attribution of Δ to an orbital splitting would not

be consistent with experiment. If the exchange splitting Δ_e of the lower state were very small the Zeeman splitting of the triplet would lead to a strong dependence of the radiative lifetime on B. A larger value of Δ_e would be manifested in the T-dependence of τ_S and in the selectively excited PL.

The PL arises from localized excitons and not from localized electrons and holes with a significant spatial separation. The theory of localized excitons accounts for the singlet radiative lifetime [3] and the exchange splitting. Separated electrons and holes, in contrast, have a much longer lifetime [21], and a much smaller exchange splitting [8] because the overlap of their envelope functions decreases exponentially with separation [8].

Our theory complements that of Vial *et al* [22], which accounts for the decrease in PL efficiency as T is increased from 300 K to 500 K, in terms of an increase in non-radiative recombination with increasing T. Our own measurements of efficiency between 2 K and 300 K show that the decline in efficiency begins at 200 K. The radiative efficiency of our material at 300 K is still high [3], and the fit of figure 2(*b*) is not significantly altered if these high-temperature non-radiative processes are taken into account.

Our results provide compelling evidence in favour of the theory that the luminescent states are quantum-confined excitons in crystalline Si. The points of agreement between this theory and experiment are

(i) the natural explanation of the size and photon-energy-dependence of τ_L, τ_U and Δ,

(ii) the number and energy of the onsets observed in PL,

(iii) the relative intensities and photon-energy-dependence of these onsets, details of which will be presented in a future publication.

In particular, the identification of momentum-conserving processes of crystalline Si shows that both the phonon *and* the luminescent exciton are located in crystalline Si and hence it provides a clear signature of the electronic bandstructure of crystalline Si.

This result shows that the exciton cannot be confined to a surface layer of different chemical composition or atomic structure, and, together with the energy upshift of the PL [1–3], and the ~ 30 Å wire width found in TEM [2], demonstrates that the luminescent states are quantum-confined excitons in crystalline Si wires. Our calculations for such excitons show that the large exchange splitting is an inevitable property of the luminescent exciton, and so the energy splitting and lifetimes that we observe can be explained naturally in terms of the simplest possible quantum-confined excitonic state.

In conclusion, our measurements show that the main PL band of porous Si arises from the recombination of localized excitons in undulating crystalline Si wires. Quantum confinement in this structure causes the large upshift of the PL energy into the visible spectrum, and the large exchange splitting of the exciton that we have observed.

References

[1]   Canham L T 1990 *Appl. Phys. Lett.* **57** 1046–8

[2]   Cullis A G and Canham L T 1991 *Nature* **353** 335–8
[3]   Read A J, Needs R J, Nash K J, Canham L T, Calcott P D J and Qteish A 1992 *Phys. Rev. Lett.* **69** 1232–5
[4]   Canham L T, Houlton M R, Leong W Y, Pickering C and Keen J M 1991 *J. Appl. Phys.* **70** 422–31
[5]   Bsiesy A, Vial J C, Gaspard F, Herino R, Ligeon M, Muller F, Romestain R, Wasiela A, Halimaoui A and Bomchil G 1991 *Surf. Sci.* **254** 195–200
[6]   Xie Y H, Wilson W L, Ross F M, Mucha J A, Fitzgerald E A, Macaulay J M and Harris T D 1992 *J. Appl. Phys.* **71** 2403–7
[7]   Hegarty J and Sturge M D 1985 *J. Opt. Soc. Am.* B **2** 1143–54
[8]   Henry C H, Faulkner R A and Nassau K 1969 *Phys. Rev.* **183** 798–806
[9]   Lane P A, Swanson L S, Shinar J and Chumbly S 1992 *Mater. Res. Soc. Symp. Proc.* **256** 169
[10] Dean P J, Haynes J R and Flood W F 1967 *Phys. Rev.* **161** 711–29
[11] Shaklee K L and Nahory R E 1970 *Phys. Rev. Lett.* **24** 942–5
[12] Stoneham A M 1975 *Theory of Defects in Solids* (Oxford: Clarendon) ch 10
[13] Permogorov S 1975 *Phys. Status Solidi* b **68** 9–42
[14] Cohen E and Sturge M D 1982 *Phys. Rev.* B **25** 3828–40
[15] Schall U, Thonke K and Sauer R 1986 *Phys. Status Solidi* b **137** 305–17
[16] Kittel C and Mitchell A H 1954 *Phys. Rev.* **96** 1488–93
[17] Faulkner R A 1969 *Phys. Rev.* **184** 713–21
[18] Merle J-C, Capizzi M, Fiorini P and Frova A 1978 *Phys. Rev.* B **17** 4821–34
[19] Sanders G D and Chang Y-C 1992 *Appl. Phys. Lett.* **60** 2525–7
[20] Canham L T, Davies G and Lightowlers E C 1985 *Proc. 13th Int. Conf. on Defects in Semiconductors* ed L C Kimerling and J M Parsey (New York: The Metallurgical Society) pp 847–53
[21] Thomas D G, Hopfield J J and Augustyniak W M 1965 *Phys. Rev.* **140** A202–20
[22] Vial J C, Bsiesy A, Gaspard F, Hérino R, Ligeon M, Muller F, Romestain R and Macfarlane R M 1992 *Phys. Rev.* B **45** 14171–6